Research Square

Preprints are preliminary reports that have not undergone peer review.
They should not be considered conclusive, used to inform clinical practice,
or referenced by the media as validated information.

Regional Hazard Assessment of Rainfall–Induced Landslide Considering Human Activity Intensity

Gang Xu
Zhejiang College of Security Technology
Xiaoqi He
Central South University
Cheng Huang
yunnan institute of geological environment monitoring
Xuexi Yang
Central South University
Qinghao Liu
1580748414@qq.com

Central South University https://orcid.org/0000-0001-9834-0676

Research Article

Keywords: rainfall-induced landslides, human activity intensity, random forests, Transformer, slope, hazard-bearing bodies

Posted Date: October 14th, 2025

DOI: https://doi.org/10.21203/rs.3.rs-7646036/v1

License: This work is licensed under a Creative Commons Attribution 4.0 International License.
Read Full License

Regional Hazard Assessment of Rainfall–Induced Landslide Considering Human Activity Intensity

Gang Xu[a,b] Xiaoqi He[c] Cheng Huang[d] Xuexi Yang[e] and Qinghao Liu[c*]

[a] Zhejiang College of Security Technology, Wenzhou 325016, China;

[b] Wenzhou Future City Research Institute, Wenzhou 325016, China;

[c] School of Geosciences and Info-Physics, Central South University, Changsha 410083, China;

[d] Yunnan Institute of Geological Environment Monitoring, Kunming, 650216, China

* Correspondence E-mail: 235001015@csu.edu.cn

Abstract: Landslide hazard assessment denotes the systematic evaluation of the likelihood of landslide occurrence within a defined temporal and spatial context. Rainfall-induced landslide hazard assessment methods often fail to adequately consider the impacts of human activities, resulting in assessments that lack sufficient accuracy to meet practical demands. This study proposes an innovative dynamic assessment model that integrates both environmental factors and triggering factors, enabling regional hazard evaluations that account for the dual spatial constraints imposed by slopes and hazard-bearing bodies. The study proposes an objective estimation model for quantifying human activity intensity, utilizing the Criteria Importance Through Intercriteria Correlation (CRITIC) method and the Entropy Weight Method (EWM). Subsequently, random forest and Transformer models were employed to perform a progressive assessment of landslide susceptibility and hazard. Specifically, the dynamic assessment of rainfall-induced landslide hazard incorporated human activity intensity and rainfall characteristics as key triggering factors. The case study carried out in Zhenyuan County indicates that the model substantially improves and significantly increases the accuracy of disaster warnings and reduces the required hazard assessment area by approximately 40.6%, offering a targeted and valuable reference for early warning systems and decision-making of rainfall-induced landslides.

Keywords: rainfall-induced landslides; human activity intensity; random forests; Transformer; slope; hazard-bearing bodies

1. Introduction

Since the Industrial Revolution, human transformation of the biosphere and ecosystem has continuously promoted the process of urbanization and industrialization [1]. Concurrently, it has triggered a series of geological and environmental problems [2]. Especially in plateau and mountainous areas, human demand for natural resources continues to accelerate along with rapid socio-economic development, leading to an increase in the tectonic vulnerability of the relevant regions, which in turn triggers a series of geologic hazards due to the synergistic effect of natural triggers such as

rainfall, earthquakes, and subsidence [3]. Landslides account for the highest proportion of geological disasters in China, causing serious economic losses and casualties every year [4][5]. Due to harsh environments characterized by complex topography and fragile geological structures, 75% of the registered geological disaster hazard points in southwest China are landslides [6][7]. Rainfall-induced landslides have long accounted for up to 95% of all landslides. Consequently, administrative departments at all levels have placed significant emphasis on the early warning and management of these disasters [8][9]. Landslide hazard is commonly defined as the probability of landslide occurrence considered within a specific spatial and temporal domain [10][11]. Accurate and timely estimation of landslide hazard can compensate for the evident shortcomings of susceptibility evaluation, particularly its weak timeliness [12][13]. Thus, hazard assessment is pivotal in regional early warning and emergency response to rainfall-induced landslides.

Generally, landslide hazard can be modeled as the synergistic effect of static spatial susceptibility and dynamic temporal inducibility [14][15]. Among them, susceptibility describes the spatial likelihood of landslides, influenced by environmental factors [14][16]. In contrast, inducibility highlights the temporal likelihood, influenced by triggering factors such as rainfall, earthquakes, and human activities [17] [18]. Effectively coupling temporal and spatial probabilities is key to understanding landslide hazards precisely. Domestic and foreign scholars primarily consider triggering factors like rainfall or earthquakes in evaluating landslide hazards. The relevant model methods can be categorized into four types: (1) Physical models, which explore the potential for landslides on slopes under various structural and causal conditions based on physical principles. It models triggering factors like rainfall and earthquakes as physical parameters to simulate landslide potential [18][19]. (2) Empirical models, which prioritize scoring or ranking landslide-influencing factors based on expert knowledge, then analyze and evaluate regional landslide hazards within the context of disaster mechanisms [20]. (3) Coupling models, which typically model susceptibility and inducibility independently and then employ multiplicative or probabilistic methods for quantitative estimation and hazard degree analysis [21][22]. (4) Machine learning models, which often utilize statistical parameters to describe the intricate nonlinear interactions between environmental factors and triggers, estimate disaster hazard levels through classification or regression techniques [23][24][25]. However, despite the development of numerous hazard assessment methods, the accuracy of existing models' assessment results requires enhancement due to insufficient consideration of human activity factors [26][27].

Frankly speaking, human activities, in the aggregate, denote the persistent and scale-heterogeneous pursuits—ranging from farming and forestry to mining, transport, and large-scale construction—by which populations sustain

themselves, advance socio-economic progress, and enhance quality of life [28]. At the micro level, human activities profoundly influence the distribution and occurrence of landslide disasters by altering land use patterns and accelerating environmental degradation. At the macro level, anthropogenic modification of land-cover trajectories coupled with the progressive erosion of ecological integrity exerts a major control on where and how often slope-failure events manifest [29][30]. Human activity intensity (HAI) denotes the level of impact exerted by human activities in a given area and serves as a crucial metric for assessing human activity levels within the natural environment [31]. Researchers have focused on quantifying and spatializing human activity intensity since its initial proposal [32][33][34][35]. However, research gaps remain regarding how human activities transform potential geological conditions into disaster events [14]. Over the past decade, urban and infrastructure development in China has accelerated, with human activities increasingly altering the geological environment. Additionally, there has been an increase in abnormal weather events, and earthquakes have become more frequent in the plateau and mountainous regions. Therefore, geological disasters are still frequent and likely to occur [6]. Consequently, rigorous quantification of human activity intensity is a prerequisite for refining the predictive fidelity of rainfall-induced landslide hazard assessment.

In recent years, the estimation methods for the intensity of human activities have primarily focused on the following aspects: On one hand, human activity intensity is statistically approximated by mapping socio-economic proxies, namely the coincident patterns of population density and GDP distribution [36] [37]. On the other hand, field surveys and expert experience are combined to conduct qualitative or semi-quantitative assessments of the types and intensity of human activities in specific regions [32][38]. However, existing methods for estimating the intensity of human activities still have some limitations. Firstly, most methods rely on socio-economic indicators or land use data. Although these indicators can reflect certain aspects of human activities, they often fail to comprehensively capture the complex impacts of human activities on the geological environment [39]. For example, some micro-level human activities, such as engineering construction and mining, may singularly initiate geological disasters, but these are difficult to reflect in macro-level socio-economic indicators. Secondly, existing methods often lack a comprehensive consideration of the interaction between natural environmental conditions and human activities when estimating HAI [40][41]. HAI is jointly influenced by natural environmental conditions and socio-economic factors; relying on a single perspective for estima-

tion may produce biased outcomes. Moreover, most existing estimation methods are subjective and dependent on experts. Variations in indicator choice and weight assignment among researchers often lead to inconsistencies, reducing the cross-regional comparability and practical applicability of estimation outcomes [42][43].

Overall, although many studies have explored methods for hazard assessment, two key challenges remain when incorporating human activity intensity into regional assessments of rainfall-induced landslides:

(1) Existing studies typically incorporate indicators based on dynamic or static rainfall into hazard assessments, with less attention given to the impact of HAI on landslide occurrence. Consequently, the insufficient consideration of independent variables leads to the accuracy of existing model assessment results still needing improvement. Therefore, any assessment model for rainfall-induced landslides should separately account for the destabilizing role of human activities[29].

(2) Accurately estimating human activity intensity has always been challenging due to the high expert dependency on indicator selection and data processing. Existing studies often only consider land cover types as basic factors, while the diversity of human activities is generally overlooked, leading to a lack of interpretability in the assessment results of rainfall-induced landslide disaster scenarios. Furthermore, how to objectively assign weights considering indicator characteristics for multi-source heterogeneous human activity basic data is also a question worthy of research.

This study is dedicated to proposing an improved assessment strategy for rainfall-induced landslide disasters by explicitly embedding the dimension of HAI, thereby advancing both the reliability and the explanatory depth of the hazard maps. Our contributions include 3 aspects: First, this study developed a model for estimating human activity intensity, integrating natural changes, economic development, and human regulation factors from a big data perspective. Second, this study used ML methods for a static susceptibility assessment of rainfall-induced landslides, and considering HAI, also developed a dynamic assessment mechanism for the rainfall-induced landslides. Third, by analyzing the dual spatial constraints of slope and bearing body, a precise evaluation of rainfall-induced landslides in Zhenyuan County, Yunnan Province, was achieved.

2. Study Area and Data

2.1 Overview of Zhenyuan County

Zhenyuan County, situated in the southwest of Yunnan Province, falls under the jurisdiction of Pu'er City. Zhenyuan County, covering an area of 4148.023 km², is positioned between 100°21′ and 101°31′ east longitude and 23°34′ and 24°22′ north latitude. The geological structure is complex. Landslide geological disasters, triggered by earthquakes,

heavy rainfall, and human engineering activities, are prevalent. Statistics show that the average annual rainfall in Zhenyuan County over the past decade has surpassed 1175 mm. A detailed investigation report reveals that 25,766 individuals and assets valued at 962.07 million yuan in Zhenyuan County are at risk from various geological disasters to varying extents [44]. Thus, conducting geological disaster hazard assessments and enhancing public awareness of disaster prevention and mitigation are crucial for ensuring stable economic development. The landslide inventory for Zhenyuan County is mapped in Figure 1.

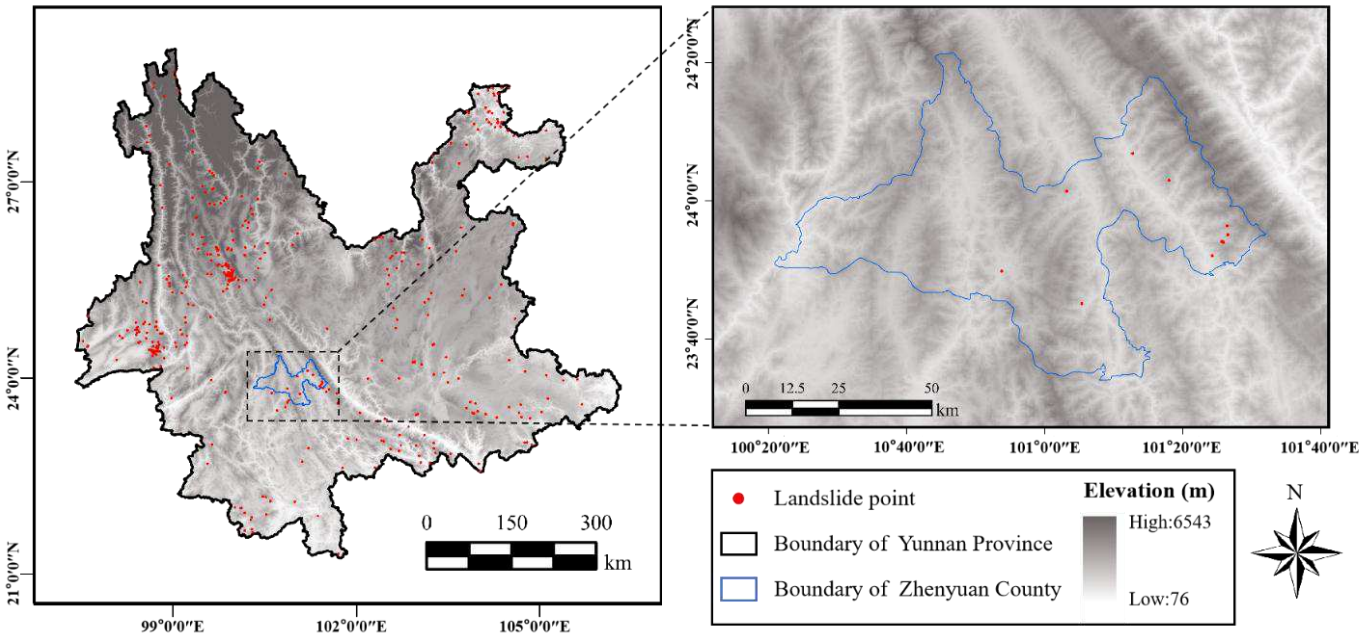


Figure 1. Distribution of the study area and historical landslide hazards.

2.2 Data Source and Pre-processing

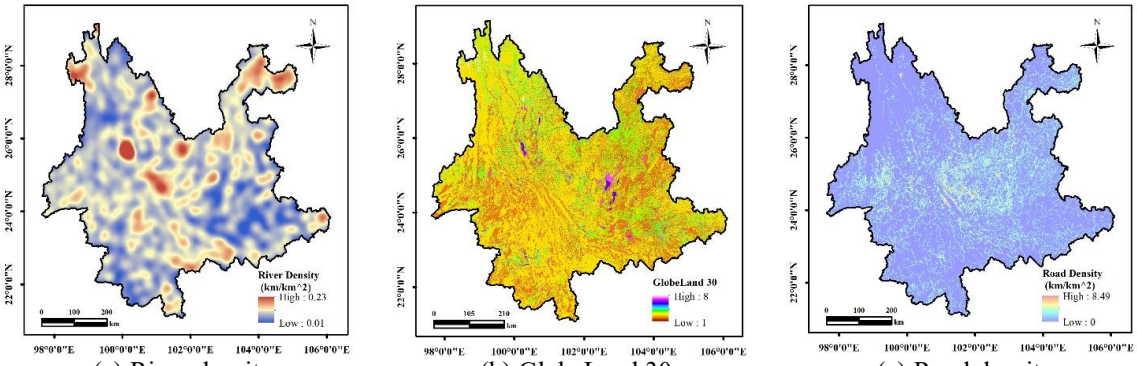
A meticulous screening process yielded 205 rainfall-induced landslide disaster events, collected from the Yunnan Provincial Institute of Geological Environment Monitoring, spanning from January 2022 to May 2024 [14]. These events are distributed across 16 prefecture-level administrative divisions in Yunnan Province. In addition, key indicators of human activities, consistent with the mechanisms of landslide occurrence and the geological context of the study region, were collected and subjected to preprocessing. Additionally, environmental factors related to topography, geological structure, and meteorological precipitation triggers were assembled and preprocessed. Overall, the research data are primarily acquired from various sensors aboard satellites (such as Landsat, Luojia-1, and meteorological radars) and from ground-based monitoring instruments. The data overview is shown in Table 1.

Table 1. Sources of topography, geological structure, human activities, and meteorological precipitation datasets.

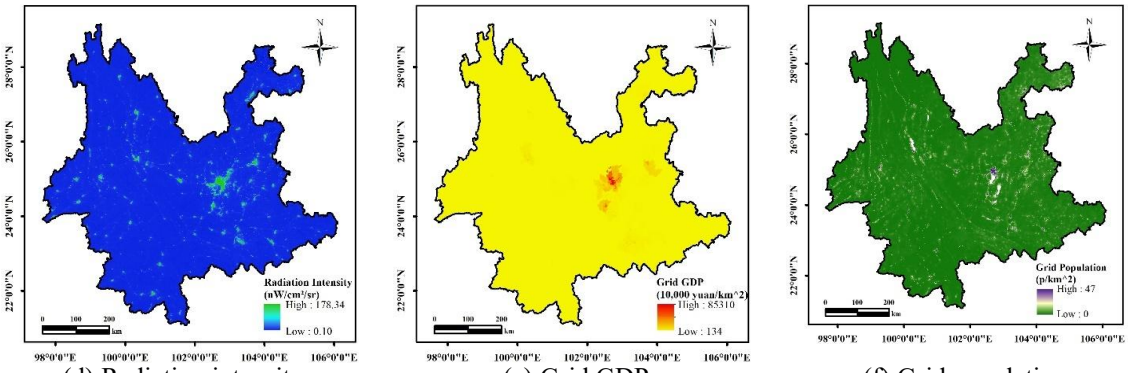
Data Types	Dataset	Data Source	Update frequency	Resolution/Scale

Topography	DEM	USGS	Almost static	30m
	Landsat-8	China Geological Survey	Almost static	30m
Geological structure	Soil Type	Chinese Academy of Sciences	Almost static	1：1000000
	Geological type	Chinese Academy of Sciences	Almost static	1：2500000
	Mining area distribution	National Mineral Deposits Database	Yearly	1：50000
	Deformation Data	European Space Agency Official Website	Quarterly	20m
	Fault distribution	Chinese Academy of Sciences	Almost static	1：2500000
Human activities	Road network and water system	NGCC	Almost static	1：250000
	Land cover data	NGCC	Every 5 years	30m
	Building outline	NGCC	Yearly	1：50000
	Population Density	WorldPop Hub	Yearly	1000m
	Night light remote sensing	Wuhan University	15 days	130m
	GDP Distribution	Chinese Academy of Sciences	Yearly	1000m
Meteorological precipitation	Daily rainfall	National Meteorological Science Data Center	Daily	1000m

Environmental factors are essential for landslide formation, dictating their scale, size, and location. Environmental and triggering factors jointly define the conditions and processes that initiate landslide disasters. Thus, the preprocessing of environmental and triggering factors is critical for assessing landslide hazard [14][20]. Through numerical cleaning, coordinate system projection, and resampling the data listed in Table 1 at a 300-meter resolution, a total of 6 human activity factors, 12 environmental factors, and 3 rainfall factors were derived. Some of these data are continuously updated, while others are rarely updated. They are used respectively to estimate the HAI, susceptibility, and the hazard level of rainfall-induced landslides. The spatial distribution of relevant factors is shown in Figures 2 to 4.

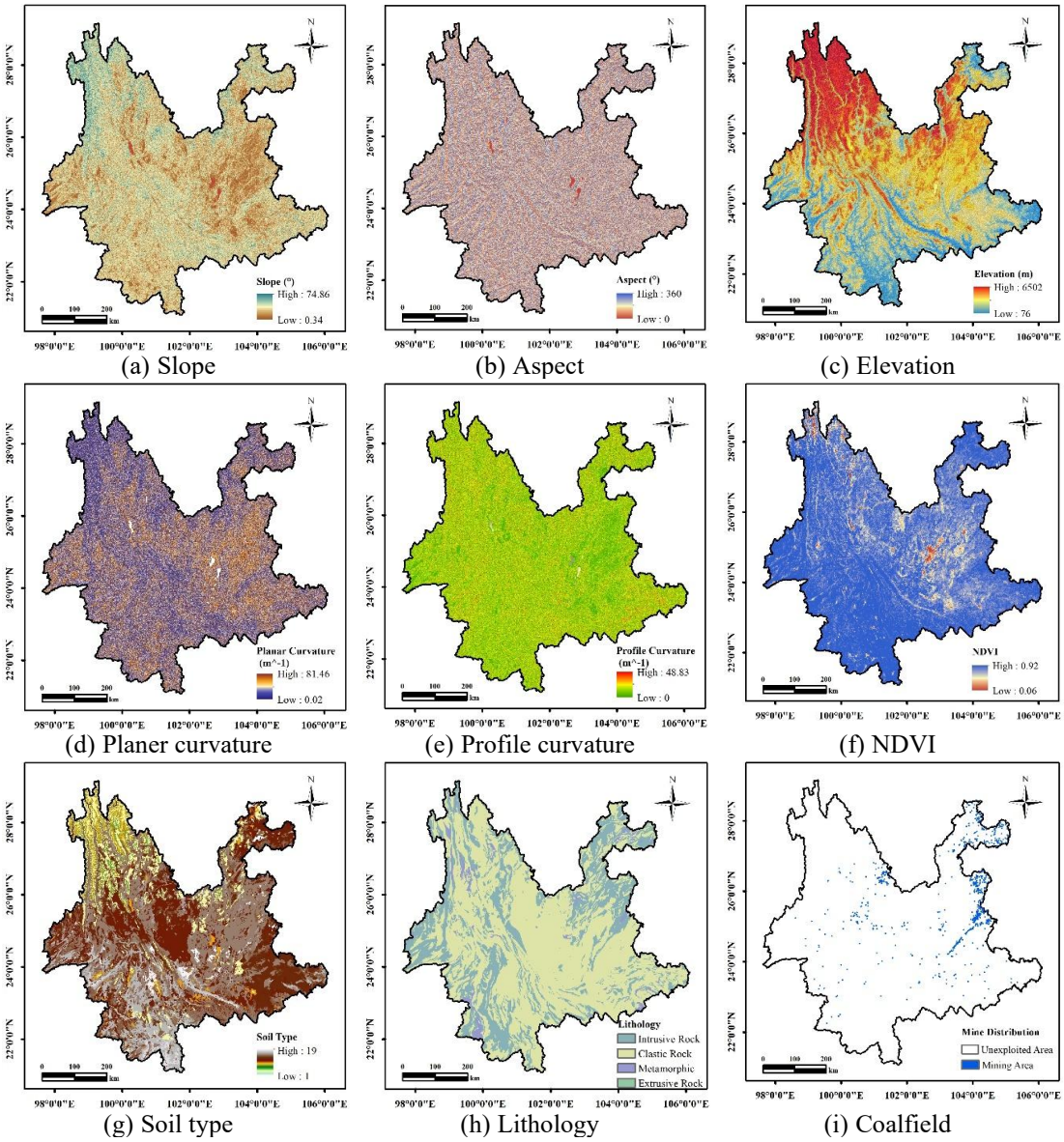


(a) River density (b) GlobeLand 30 (c) Road density



(d) Radiation intensity (e) Grid GDP (f) Grid population

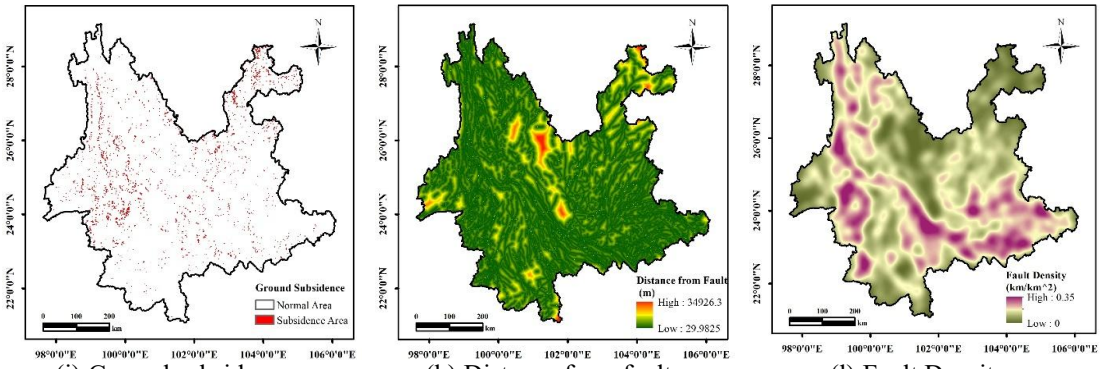
Figure 2. Distribution of six human activity factors in the province.



(a) Slope (b) Aspect (c) Elevation

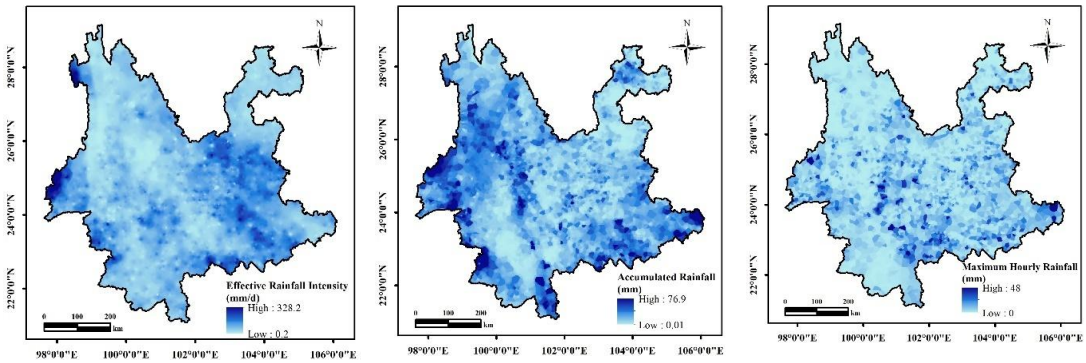
(d) Planer curvature (e) Profile curvature (f) NDVI

(g) Soil type (h) Lithology (i) Coalfield



(j) Ground subsidence (k) Distance from fault (l) Fault Density

Figure 3. Distribution of 12 environmental factors in the province



(a) Historical 7-day effective rainfall intensity (b) Total rainfall for the day (c) Maximum hourly rainfall for the day

Figure 4. Distribution of rainfall trigger factors across the province (August 8, 2023).

3. Methods

In this study, a 300-meter grids were employed as the fundamental analysis unit, incorporating multiple environmental and triggering factors to assess the hazard of rainfall-induced landslides. Specifically, human activity intensity was objectively estimated and integrated into the dynamic hazard evaluation as a key triggering factor. The model framework is illustrated in Figure 5. The primary contributions of this study are summarized in three aspects: First, an objective weighting method was developed to enable a comprehensive estimation of human activity intensity. Second, the landslide susceptibility and hazard levels at the provincial scale were quantified through random forest and Transformer models. Finally, the optimization of hazard assessment results was conducted through the implementation of dual spatial constraints based on slope and hazard-bearing body. Furthermore, a visual analysis of the hazard assessment outcomes in Zhenyuan County was performed based on the case study.

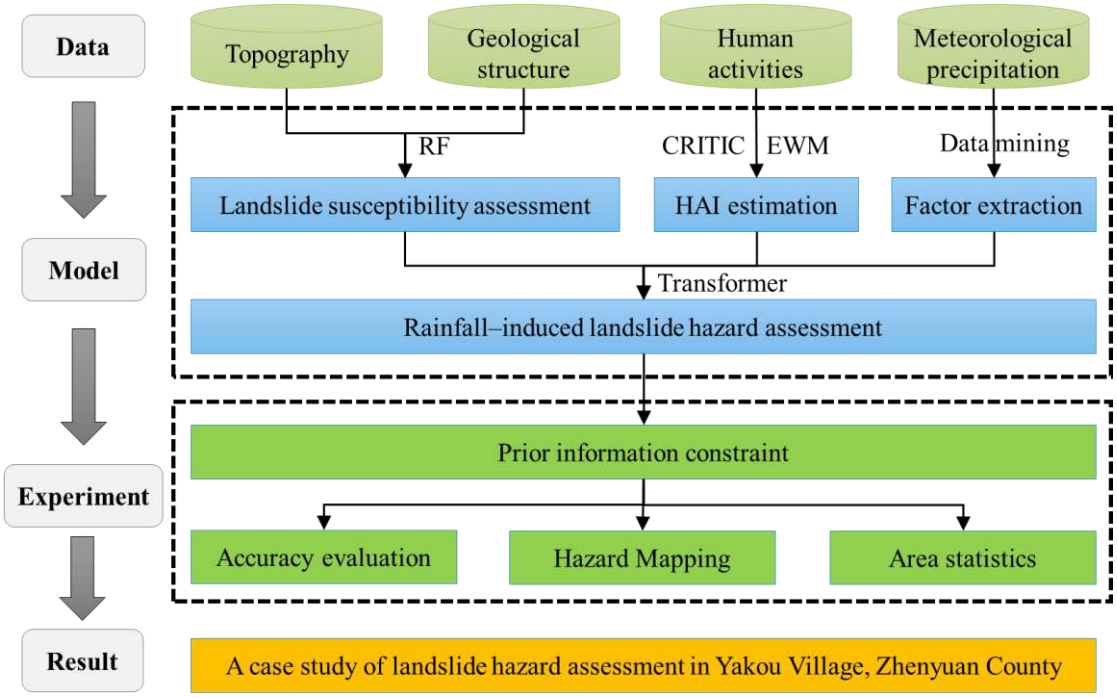


Figure 5. Framework of a regional rainfall-induced landslide hazard assessment model considering the intensity of human activities.

3.1 Quantification of Human Activity Intensity

Criteria Importance Through Intercriteria Correlation (CRITIC) is an objective weighting method proposed by Diakoulaki in 2015 [45]. The core idea is to determine the objective weight of each indicator by assessing both its comparative strength and its inter-indicator conflict [46]. Comparative strength is indicated by the standard deviation of the evaluation indicator, reflecting the variation in values across different schemes. Indicator conflict is indicated by the correlation coefficient, reflecting the similarity among different indicators. A larger standard deviation signifies greater fluctuation in indicator values across schemes, thereby assigning a higher weight. Conversely, a stronger correlation indicates less conflict between indicators, resulting in a lower weight. The CRITIC method considers the variability within each indicator and the correlation between them [47]. This method leverages the objective attributes of the data for evaluation [45]. The CRITIC method encompasses the following steps for implementation.

(1) Dimensionless processing. Assuming that there are m sample units to be evaluated and n measurement indicators, by normalizing the original data to the maximum and minimum values, the indicator value of each sample can be expressed as a matrix X, as shown in Formula 1.

$$X = \begin{bmatrix} x_{11} & \cdots & x_{1n} \\ \vdots & \ddots & \vdots \\ x_{m1} & \cdots & x_{mn} \end{bmatrix} \quad (1)$$

(2) Indicator calculation. The indicator comparison strength and the conflict between indicators are estimated by calculating the standard deviation σ_j of the j th indicator and the correlation coefficient R_j between indicators, as shown in formulas (2) to (4). Among them, $\overline{x_j}$ represents the data mean of the j th indicator, x_{ij} represents the normalized value of the j th indicator of the i th sample unit, and r_{jk} represents the Pearson correlation coefficient between the j th indicator and the k th indicator.

$$\overline{x_j} = \frac{1}{m}\sum_{i=1}^{m} x_{ij} \tag{2}$$

$$\sigma_j = \sqrt{\frac{\sum_{i=1}^{m}\left(x_{ij} - \overline{x_j}\right)^2}{m-1}} \tag{3}$$

$$R_j = \sum_{k=1}^{n}\left(1 - r_{jk}\right) \tag{4}$$

(3) Weight calculation. The information volume c is the comprehensive value of the index conflict and index comparison and is also the core embodiment of the CRITIC objective weighting method. Based on the information volume c, the preliminary weight w of index j can be calculated, as shown in formula (5) to formula (6):

$$C_j = \sigma_j \times R_j \tag{5}$$

$$w_j = \frac{C_j}{\sum_{j=1}^{n} C_j} \tag{6}$$

The Entropy Weight Method (EWM) originates from the "information theory" framework, introduced in 1948 [48]. The essence of the entropy weight method is to assess the uncertainty and randomness of decision-making indicators via their information entropy [49]. Higher information entropy in an indicator indicates more dispersed information, reducing its distinctiveness and impact on decision-making. Conversely, lower entropy signifies more concentrated information, amplifying its distinctiveness and decision-making influence. The entropy weight method's advantage lies in its ability to objectively determine indicator weights based on data distribution [50][51]. This approach eliminates subjective bias in weight assignment. The entropy weight method involves the following steps for implementation:

(1) Information entropy calculation. Calculate the weight of each sample unit under each indicator, and then use the information entropy formula to calculate the information entropy of each indicator. Among them, f_{ij} represents

the weight of the i th sample unit under the j th indicator, Q_j represents the entropy value of the j th indicator, Qw_j represents the entropy weight of the j th indicator, and the value range of Q_j and Qw_j is (0,1], as shown in formulas (7) to (9).

$$f_{ij} = \frac{r_{ij}}{\sum_{i=1}^{m} r_{ij}} \tag{7}$$

$$Q_j = -\frac{1}{\ln m}\sum_{i=1}^{m}\left(f_{ij} \times \ln f_{ij}\right) \tag{8}$$

$$Qw_j = \frac{1-Q_j}{\sum_{j=1}^{n}\left(1-Q_j\right)} \tag{9}$$

(2) Weight optimization. The CRITIC method determines objective weights by accounting for both the comparability within a single indicator and the conflicts across different indicators, thereby exploiting the inherent characteristics of the data while preserving its informational content. However, the single CRITIC method lacks consideration of the differences in the importance of indicators. Integrating indicator weights with their corresponding entropy values enables a more comprehensive reflection of inter-indicator comparability, conflicts, and relative importance. Therefore, this work proposes a combined weighting model that couples CRITIC and entropy values. The calculation method is shown in formula (10).

$$W_j = \left(1+\beta^2\right) \times \frac{w_j \times Qw_j}{\left(\beta^2 \times w_j\right) + Qw_j} \tag{10}$$

Among them, w_j represents the initial weight w_j of indicator j , and the reconciliation parameter β represents the multiple of the importance of the contrast and conflict between indicators compared with the reference value of the indicator importance, which has important physical significance. Usually β is 0.5, 1, or 2.

(3) Calculation of HAI. Based on the optimization weights obtained by formula (10) and the driving data of each sample unit, the human activity intensity P_i of each sample unit can be further calculated using formula (11). The workflow for quantifying human activity intensity is shown in Figure 6.

$$P_i = \frac{1}{n}\sum_{j=1}^{n} W_j \times x_{ij} \tag{11}$$

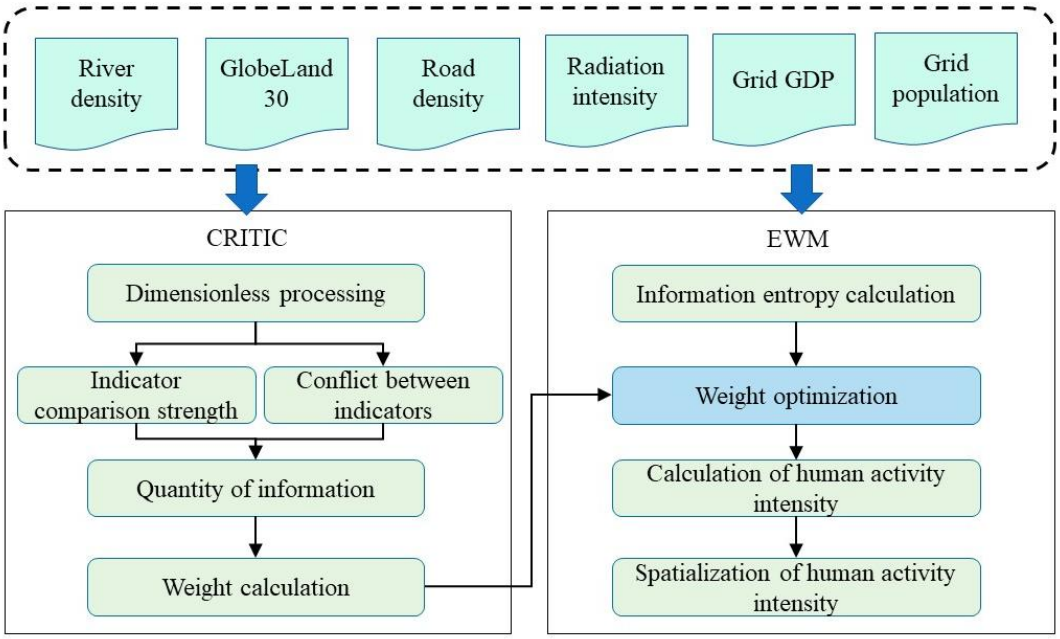


Figure 6. The workflow for quantifying human activity intensity by coupling CRITIC and EWM.

3.2 Random Forest for Susceptibility Assessment

The random forest model employs multiple classification trees to establish a nonlinear relationship between data features and labels, suitable for both classification and regression tasks [52]. The model generates decision trees that reflect the distribution of a sampled subset of the training data through sampling with replacement [53][54]. It then aggregates the classification outcomes of all trees, voting, and scoring to determine the optimal classification result. The randomness in the random forest is manifested in two ways: random feature selection and random sampling of data [55]. While the trees in a random forest share certain characteristics, they also differ from one another, enabling the model to effectively handle high-dimensional datasets without additional dimensionality reduction [56]. A potential drawback of the random forest model is its susceptibility to overfitting when dealing with noisy classification problems [52]. The essence of rainfall-induced landslide susceptibility assessment lies in estimating the vulnerability level of the target area based on geographical similarity, which is consistent with the characteristics of small sample sizes and non-linear modeling [14][20]. Random forest models are adept at capturing nonlinear decision boundaries and are highly tolerant of outliers and noise. Hence, a random forest approach was applied in this work to assess the susceptibility of landslides.

The random forest method uses impurity to measure the best split and calculates the factor importance through the reduction value D_{Gk} of the Gini index of factor index k when the node is split [20]. The proportion of the average Gini

index reduction value to the total average Gini index reduction value of all factors is P_k, and the calculation method is shown in formula (12):

$$P_k = \frac{\sum_{h=1}^{n}\sum_{j=1}^{t} D_{Gkhj}}{\sum_{k=1}^{m}\sum_{h=1}^{n}\sum_{j=1}^{t} D_{Gkhj}} \tag{12}$$

Where m is the total number of factors, n is the number of classification trees, and t is the number of nodes in a single tree, respectively.; D_{Gkhj} is the Gini index reduction value of the k th factor on the j th node of the h th tree; P_k is the importance of the k th factor [57].

3.3 Transformer for Hazard Assessment

As a deep learning framework built upon self-attention, the Transformer can accurately represent complex and nonlinear interactions between different feature variables [58]. It is particularly suitable for tasks that require modeling intricate interactions among features. The model's effectiveness stems from its self-attention mechanism, which dynamically redistributes weights by measuring inter-element correlations within the sequence, thereby enhancing its capacity to capture extended and nonlinear dependencies. The specific formula is as follows:

$$Attention(Q, K, V) = soft\max(\frac{QK^T}{\sqrt{d_k}})V \tag{13}$$

Where Q, K, and V are the query, key, and value matrices, respectively, derived from the input data through linear transformations. d_k is the dimension of the key vectors. The Softmax function normalizes the attention scores so that their sum is 1. The output is a weighted sum of the value vectors based on the attention scores. Through this mechanism, the Transformer model dynamically adjusts the importance of features and captures complex nonlinear relationships between them. The working principle of the Transformer model used for hazard assessment is shown in Figure 7.

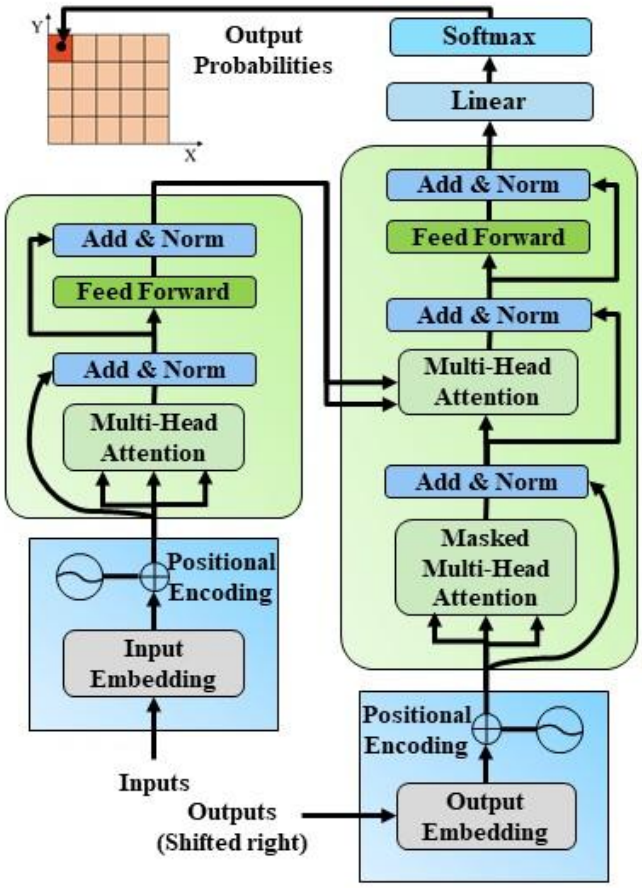


Figure 7. The working principle of the Transformer model used for hazard assessment.

Hazard assessment typically involves complex nonlinear interactions between multiple factors, such as environmental conditions, rainfall, and human activity intensity [59]. The Transformer model, with its self-attention mechanism, dynamically adjusts feature weights to efficiently identify key factors and their relationships, thereby improving the accuracy of hazard predictions. Additionally, the Transformer model can be easily extended to accommodate different hazard assessment scenarios. Therefore, the Transformer model, with its strong nonlinear modeling capabilities and efficient handling of high-dimensional data, is an ideal choice for hazard assessment.

3.4 Evaluation Indicator

To ensure a rigorous evaluation of hazard assessment outcomes, four performance metrics—accuracy, recall, false negative rate, and false positive rate—were employed to evaluate model quality. Accuracy (A) refers to the fraction of samples classified correctly out of the entire dataset. Recall (R) quantifies the correctly recognized positives compared with the overall number of positives. The false negative rate (FNR) indicates the proportion of positives wrongly assigned to the negative class, whereas the false positive rate (FPR) reflects the proportion of negatives incorrectly labeled as positives. The detailed expressions of these indicators are given in Equations (14) to (17).

$$A = \frac{TP + TN}{TP + FP + TN + FN} \tag{14}$$

$$R = \frac{TP}{TP + FN} \tag{15}$$

$$FNR = \frac{FN}{TP + FN} \tag{16}$$

$$FPR = \frac{FP}{FP + TN} \tag{17}$$

Depending on the specific needs of disaster management, there may be different focuses on the above indicators. Specifically, *R* and *FNR* focus more on the model's ability to recognize landslide hazards. At the same time, *A* and *FPR* provide a perspective on the overall performance of the model and the extent of false alarms. If avoiding underreporting (i.e., reducing casualties and property damage) is a top priority, then *R* and *FNR* will be key metrics for evaluating model performance. Conversely, if resources are limited and unnecessary precautions need to be avoided, then *FPR* will be an important consideration.

4. Experiments and Results

4.1 Human Activity Intensity Estimation

Complex topography renders existing methods for estimating human activity intensity inadequate for large-scale, refined quantitative calculations in plateau and mountainous regions [60]. Furthermore, existing methods for estimating human activity intensity are subjective and reliant on expert knowledge for indicator selection and weight assignment, hindering their widespread adoption across different regions [32]. To address these limitations, an integrated human activity indicator system is proposed, encompassing "natural transformation-economic development-human regulation" factors. Subsequently, an objective model for estimating human activity intensity is developed using CRITIC and EWM. Natural transformation, economic development, and human regulation factors reflect the phased impact of human activities on the geological environment from the perspectives of the past, present, and future [61]. Objective estimation of human activity intensity is achieved in this section by leveraging multi-source geographic big data.

Utilizing the combined weighting method outlined in Section 3.1, the weights of the 6 human activity factors are presented in Table 2. Based on the weights of each factor, the human activity intensity across Yunnan Province is calculated and visualized in Figure 8.

Table 2. Weights for 6 human activity factors (two decimal places).

Factor Name	Initial weight	Entropy Weight	Optimize weights
River density	0.39	0.09	0.14
GlobeLand 30	0.33	0.25	0.28
Road density	0.19	0.19	0.19
Radiation intensity	0.03	0.1	0.05
Grid GDP	0.06	0.17	0.08
Grid population	0.01	0.21	0.02

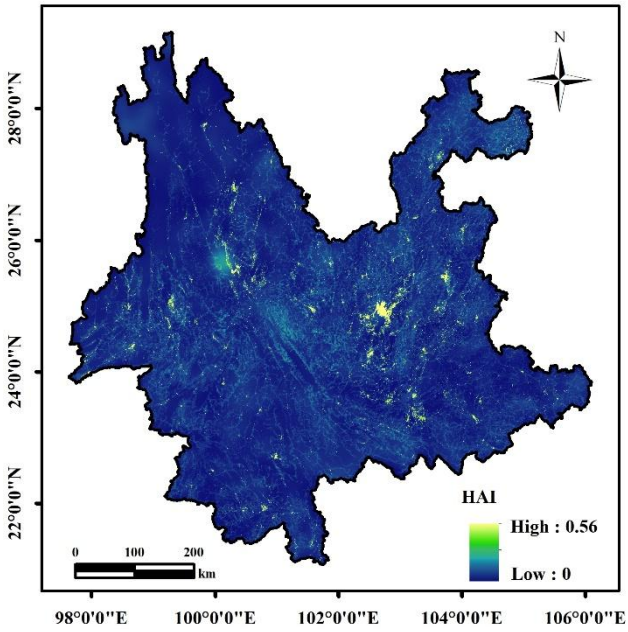


Figure 8. Spatial distribution of human activity intensity in Yunnan Province.

4.2 Landslide Susceptibility Assessment

In applying the random forest algorithm, the reliability of the dataset plays a decisive role in determining both model accuracy and generalization ability [20]. For landslide susceptibility analysis, the dataset was constructed with two categories: landslide occurrences (positive samples) and non-occurrences (negative samples). Each record includes twelve environmental attributes as inputs, with binary outputs coded as 1 for landslide sites and 0 for stable areas. To mitigate sample imbalance, a ratio of 1:2 between positive and negative cases was adopted, resulting in 615 instances. Following standard practice, the dataset was randomly divided into training (70%) and testing (30%) subsets [62]. This procedure produced a dataset reflecting regional geological and environmental conditions, which was subsequently used for model learning and validation. In the prediction stage, the trained random forest was applied to gridded spatial units, where environmental attributes were preprocessed as input features. The model then outputs susceptibility probabilities ranging from 0 to 1 for each grid cell.

In susceptibility evaluation modeling, the random forest model's key parameters are configured as follows: n_estimators set to 200, max_depth to 8, max_features to auto, and the information gain threshold to 0.025. This study utilizes

the Gini index to determine the significance of various environmental factors. The model training's factor importance ranking is as follows: elevation, fault density, soil type, surface deformation, planar curvature, profile curvature, fault distance, and slope. Factors not listed are omitted due to their importance falling below the predefined information gain threshold.

Following the random forest training principles described in Section 3.2, a detailed assessment of landslide susceptibility in Yunnan Province was performed. The spatial distribution of rainfall-triggered landslide susceptibility is illustrated in Figure 9. As shown, susceptibility values range from 0.1 to 0.87, with highly susceptible zones concentrated mainly along road corridors at higher elevations.

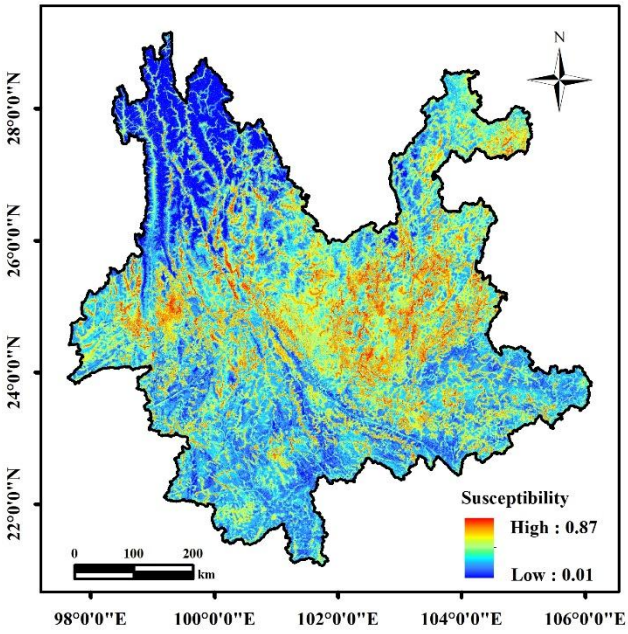


Figure 9. Spatial distribution of rainfall-induced landslide susceptibility in Yunnan Province.

4.3 Landslide Hazard Assessment

Sections 4.1 and 4.2 presented the spatial distribution of HAI and rainfall-induced landslide susceptibility. Furthermore, the Transformer model was employed to construct a hazard assessment model. Due to the limited historical landslide disaster samples available in Zhenyuan County, which makes it challenging to support effective modeling with the Transformer model, this study opted to use a dataset extracted from the entire province for training. Furthermore, to control the effectiveness of the model in the hazard prediction task for Zhenyuan County, the hazard assessment samples did not consider historical rainfall-induced landslide data from Zhenyuan County. As depicted in Figure 4, the hazard assessment samples incorporate dynamic rainfall characteristics for specific dates, not just simple features like average annual rainfall. The model's training results indicate a test set accuracy of 91.87%, a recall rate of 80.85%, a

missed rate of 19.15%, and a false alarm rate of 1.32%, suggesting that the hazard assessment model's training is highly effective.

4.4 Slope and Bearing Body Constraints

To enhance the precision of the hazard assessment further, the slope and the distribution of the hazard-bearing body are utilized as prior information for the hazard assessment. By imposing prior information constraints, unnecessary areas in the original hazard zoning can be corrected. The final hazard level for rainfall-induced landslides is articulated in formula (18).

$$H_c = H \times S_c \times B_c \tag{18}$$

In the formula, H_c and H represent the probability of hazard assessment after and before prior information constraint, respectively. S_c represents the attribute value of the slope constraint layer. Research has indicated that 95% of rainfall-induced landslides are mainly distributed in the slope range of 8°~45°, and some disaster points are located outside the slope range [63]. Based on these findings, the slopes of historical disaster points in Yunnan Province are sorted and counted, with areas having a slope of 8°~45° assigned a value of 1 and the rest assigned a value of 0. B_c represents the attribute value of the hazard-bearing body constraint layer. Buildings and roads are selected as hazard-bearing bodies. In line with existing research [64], the road network distance and building distance are reclassified with a threshold of 500 meters, assigning a value of 1 to the buffer area and 0 to all other areas. Therefore, the constraint layer of Zhenyuan County is shown in Figure 10, where the slope constraint area and the hazard-bearing area represent the range where the hazard assessment results are retained.

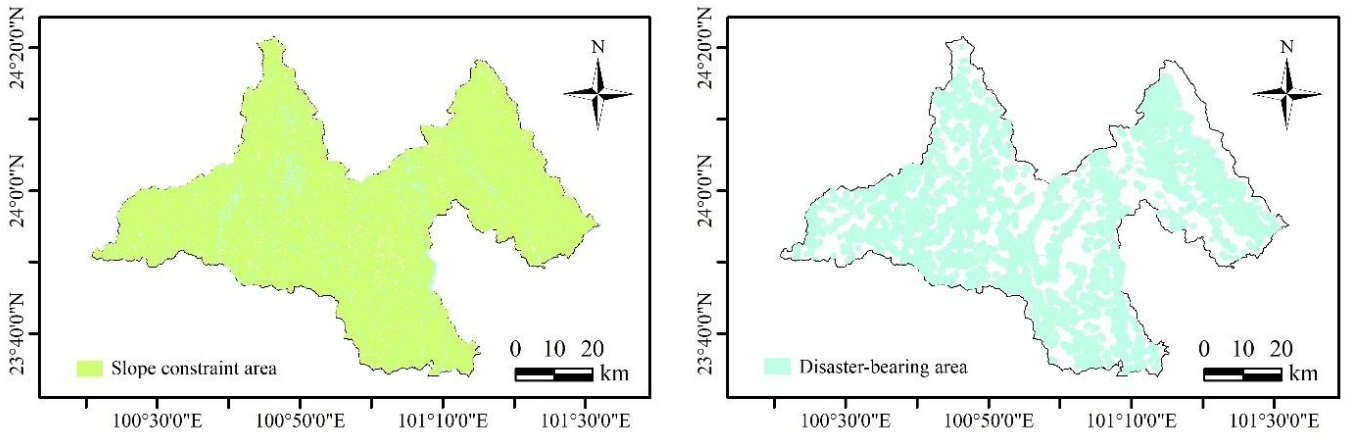


Figure 10. Spatial constraint layers of slope (a) and hazard-bearing body. (a)Slope constraint layer, (b) Hazard-prone body constraint layer.

According to the Transformer model, the hazard assessment results on August 8, 2023, are shown in Figure 11(a). Furthermore, by applying spatial constraints through formula (18), optimized hazard assessment results were obtained, as depicted in Figure 11(b). Considering the simplicity of result display, statistical rationality, and practical applicability in specific regional environments, the hazard assessment results were divided into five levels using the equal interval method: very high, high, medium, low, and very low. By comparing Figure 11(a) and Figure 11(b), it is evident that significant spatial constraints have been applied to the evaluation results at different levels. Consequently, the area of the hazard assessment results has been reduced by 49%, 34.4%, 33.5%, 20.5%, and 16% respectively, with the total evaluation area decreasing by 40.6%. The statistical results are shown in Figure 12.

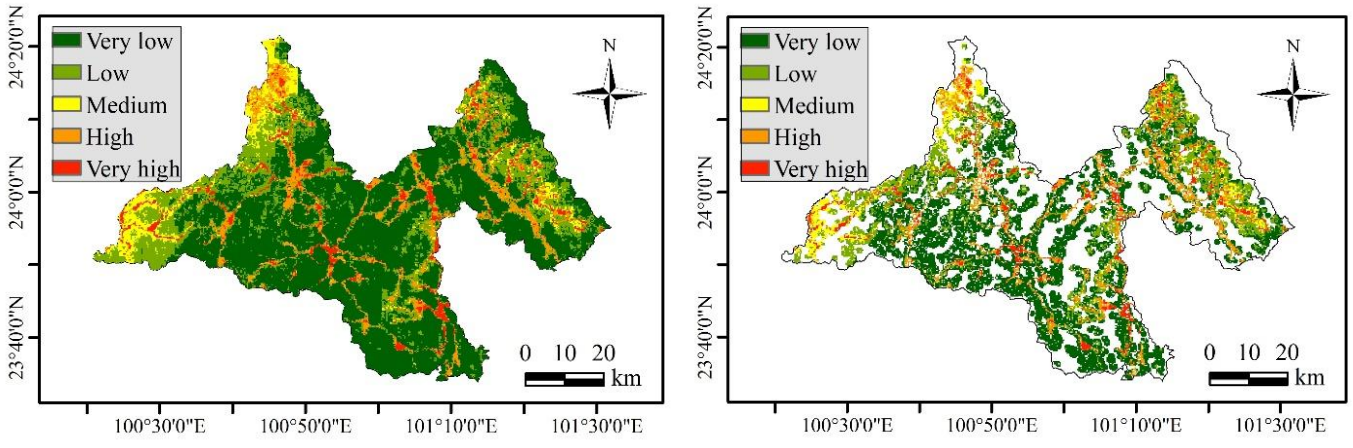


Figure 11. Hazard assessment results before (a) and after (b) prior information constraints (August 8, 2023). Evaluation results before prior information constraints, (b) Evaluation results after prior information constraints.

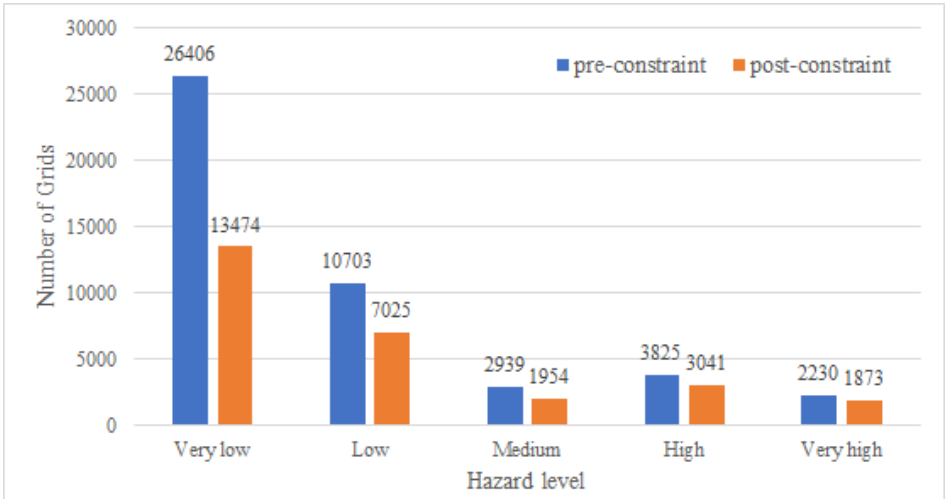


Figure 12. Changes in the hazard statistics based on prior information constraints (August 8, 2023)

4.5 Case Study of Rainfall-Induced Landslide Associated with Human Activity

The study utilizes Zhenyuan County, Yunnan Province, as a case example to carry out landslide disaster hazard assessment and mapping for a rainfall-induced landslide event that occurred in the county in recent years. The event

occurred at 4 a.m. on August 8, 2023, in Yakou Village, Heping Town, Zhenyuan County. The event was triggered by natural rainfall and was classified as a minor disaster. The traction landslide caused damage to the pigpen on the upper side of the farm, resulting in direct economic losses and family property losses totaling 200,000 yuan. Figure 13 shows an aerial view of the geographical location of the Yaokou landslide.

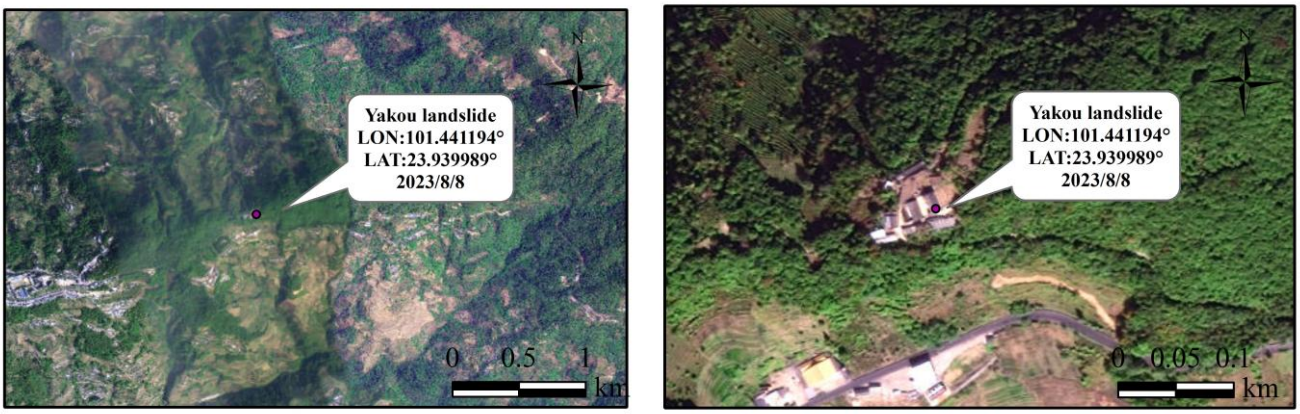


Figure 13. Geographic location of the Yaokou landslide. (a) Aerial view of the Yaokou landslide as seen from remote sensing imagery, (b) Detailed version of the aerial view of the Yaokou landslide.

To analyze the early warning performance of the model, the hazard assessment results from August 8, 2023, were spatially visualized. According to the hazard probability level of the landslide location in Figure 14 (a) and Figure 14 (b), it can be inferred that a more accurate hazard is obtained by considering HAI. The main basis is that considering the intensity of human activities can classify the grid unit where the event is located as a high hazard level, and this result can directly trigger the preset disaster early warning mechanism. In particular, River density, land cover type, Road density, Radiation intensity, Grid GDP, and Grid population were considered comprehensively and objectively in the estimation process of HAI. However, Figure 14 (b) does not consider HAI, directly weakening the modeling of human activity triggering factors, and thus obtaining an evaluation result with a lower degree of danger. The evaluation model that incorporates HAI, as proposed in this study, proves to be a more suitable approach for assessing the hazards of rainfall-induced landslides.

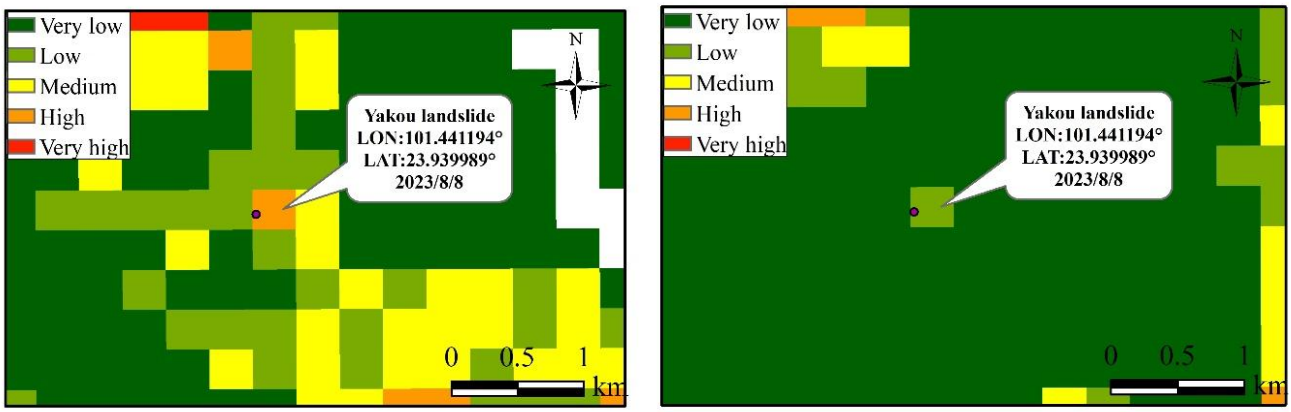


Figure 14. Hazard assessment results of Zhenyuan County. (a) Hazard assessment result considering the intensity of human activities, (b) Hazard assessment result without considering the intensity of human activities.

5. Discussion

5.1 Comparison with Existing Work

In the realm of landslide hazard assessment, prior research has predominantly focused on natural factors such as rainfall intensity, slope gradient, and soil properties, often neglecting the significant role of human activities [65]. Although previous studies have established a strong basis for understanding natural triggers of landslides, they have not fully addressed the role of human activities, which are now widely acknowledged as significant drivers of landslide hazards [14]. For instance, many existing models rely on subjective weighting methods to quantify human activity intensity, leading to potential biases and a lack of robustness in the assessment results [32][33]. In contrast, this study innovatively integrates the CRITIC and EWM objective weighting models, leveraging multi-source geographical big data to provide a more objective and comprehensive estimation of HAI. This approach not only addresses the limitations of previous studies but also offers a more nuanced understanding of how human activities interact with natural factors to influence landslide hazard [34][35][14].

Furthermore, traditional landslide hazard assessment methods often suffer from a lack of spatial precision and efficiency, resulting in overly broad hazard classifications that may not accurately reflect the true hazard distribution [20]. The spatially constrained assessment strategy employed in this study, which incorporates slope distribution and disaster-bearing body distribution, represents a significant advancement. By applying dual spatial constraints, this study effectively reduces the assessment area, and the hazard assessment areas at different levels were reduced by 49%,

34.4%, 33.5%, 20.5%, and 16% respectively, thereby enhancing the precision and efficiency of the hazard mapping process. This is a notable improvement over previous methods that fail to account for the spatial heterogeneity of landslide hazards, often leading to inefficient allocation of resources and inadequate disaster preparedness [18][22][23].

5.2 Strengths and Limitations of the Proposed Strategy

The proposed strategy in this study offers several distinct advantages over existing approaches. Firstly, the integration of human activity intensity into the landslide hazard assessment model significantly enhances the model's ability to capture the complex interactions between human activities and natural processes. By considering factors such as river density, land cover type, road density, radiation intensity, grid GDP, and grid population, the model provides a more holistic view of the hazard landscape. The adoption of this holistic method not only raises the reliability of hazard predictions but also ensures that the model captures real-world contexts in which human impacts act as major triggers for landslides [2][14]. Moreover, the use of objective weighting models ensures that the relative importance of each factor is accurately determined, thereby reducing the subjectivity associated with traditional weighting methods [36][37][38].

However, despite these strengths, the proposed strategy also has its limitations. One major limitation is the resolution of the data used in this study. Although a 300 m grid provides adequate support for regional-scale assessments, it fails to reflect detailed variations in landslide processes [19]. This limitation is particularly evident when the assessment results are spatially overlaid with actual landslide events, where higher-resolution data would be necessary to fully capture the nuances of the hazard distribution. Additionally, the current study relies on a relatively small dataset of 205 rainfall-induced landslide cases for model training. Although the dataset was curated with attention to quality, its relatively small scale could constrain the model’s generalization capacity across different regions or application contexts. Furthermore, the complexity of human activities means that the current indicator system for human activity intensity, although comprehensive, may still need further refinement to fully account for the multifaceted nature of human influences on landslide hazards [14].

5.3 Innovation and Future Prospects

The innovation of this study lies in its novel approach to integrating human activity intensity into landslide hazard assessment through the use of objective weighting models and multi-source geographical big data. This integration represents a significant departure from traditional methods that often treat human activities as secondary factors [26].

This study highlights human activities as a key driver of landslide hazards, offering fresh perspectives on the intricate interactions between human and natural systems. By strengthening assessment accuracy and robustness, the proposed strategy further supports effective understanding and governance of landslide hazards in environments where human activity plays a major role [7][29].

Looking ahead, the potential applications of this study are extensive. The proposed strategy can be adapted and applied to various regions with different environmental and socio-economic characteristics, providing valuable support for disaster risk management, urban planning, and ecological conservation [9][19]. In particular, the ability to quickly update and dynamically adjust hazard assessments based on real-time data makes this method highly suitable for use in emergency response and early warning systems [13]. Future work will focus on further refining the human activity intensity indicator system to incorporate additional factors and perspectives. Additionally, efforts will be made to collaborate with relevant authorities to validate the assessment results in different geographical contexts and to explore the potential for integrating this method with other advanced technologies such as machine learning and remote sensing. Ultimately, the goal is to develop a more comprehensive and accurate landslide hazard assessment framework that can better serve the needs of both scientific research and practical applications.

6. Conclusions

A regional rainfall-induced landslide hazard assessment incorporating the intensity of human activities was conducted. First, the CRITIC and EWM methods were used to generate an objective, spatially explicit measure of HAI over a large region. Subsequently, random forest and transformer models were used to assess landslide susceptibility and hazard in Zhenyuan County, Yunnan Province. Furthermore, spatial constraints for rainfall-induced landslide hazards were imposed by incorporating slope and hazard-bearing body information. The case study of Zhenyuan County, Yunnan Province, demonstrated that: (1) The index system was constructed using three types of human activity geographic data, namely natural transformation, economic development, and humanistic regulation. The estimated human activity intensity can reveal the laws of human activities in a more detailed, comprehensive, and objective manner. (2) By incorporating slope and hazard-bearing body constraints, the hazard assessment model can reduce the number and area of grid cells across various hazard levels while minimizing underreporting. (3) When the intensity of human activities is considered, the early warning capacity of the assessment improves, and the hazard levels align more closely with the actual occurrence of landslide events.

In summary, the study offers multiple contributions. First, the intensity of human activities is quantitatively estimated at a fine scale by incorporating geographic data, including natural transformation, economic development, and human regulation. Second, the dynamics of rainfall-induced landslide hazard were assessed by integrating human activity intensity data with rainfall-triggering factors. Additionally, the impact of HAI and spatial constraints on hazard modeling outcomes was explored through control experiments. This information can help guide disaster prevention and control. Thus far, the research has addressed the key question posed in the introduction: how the intensity of human activities is spatially distributed and its influence on the effectiveness of rainfall-induced landslide hazard assessment. In future work, further comparisons with meteorological risk warning or other methods will be conducted to thoroughly discuss the feasibility and applicability of this approach.

Author Contributions: All authors have read and agreed to the published version of the manuscript.

Funding: Not applicable.

Institutional Review Board Statement: Not applicable.

Informed Consent Statement: Not applicable.

Data Availability Statement: Not applicable.

Competing Interests: All authors certify that they have no affiliations with or involvement in any organization or entity with any financial interest or non-financial interest in the subject matter or materials discussed in this manuscript.

References

[1] Qin, D. Climate change science and sustainable development. *Progress in Geography*, 2014, 33(7), 874-883.

[2] Cardinale, B.; Duffy, J.; Gonzalez, A.; ... & Naeem, S. Biodiversity loss and its impact on humanity. *Nature*, **2012**, *486*(7401), 59-67.

[3] Tyagi, A.; Tiwari, R.; James, N. A review on spatial, temporal and magnitude prediction of landslide hazard. *Journal of Asian Earth Sciences*: *X*, **2022**, *7*: 100099.

[4] Zhang, S.; Wang, Y.; Jia, B.; Zhao, S. Spatial-temporal changes and influencing factors of geologic disasters from 2005 to 2016 in China. *Journal of Geo-information Science*, **2017**, *19*(12):1567-1574.

[5] Huang, R. Large-scale landslides and their occurrence mechanisms in China since the 20th century. *Journal of Rock Mechanics and Engineering*, **2007**, (03): 433-454.

[6] Department of Natural Resources of Yunnan Province, Yunnan Province Geological Hazard Prevention and Control '14th Five-Yea r Plan' (2021-2025) [EB]. https://dnr.yn.gov.cn/html/2022/dizaifangzhi_0830/33678.html, (accessed 24 June 2024).

[7] Xu, Q. Understanding and Consideration of Related Issues in Early Identification of Potential Geohazards. *Geomatics and Information Science*

of Wuhan University, **2020**, *45*(11):1651-1659.

[8] Ministry of Natural Resources of the People 's Republic of China. National Geological Hazard Prevention and Control "14th Five -Year Plan" [EB]. https://www.gov.cn/zhengce/zhengceku/2023-01/04/content_5734957.htm, (accessed 24 December 2023)

[9] Xu, Q. Understanding the landslide monitoring and early warning: Consideration to practical issues. *Journal of Engineering Geology*, **2020**, *28*(2): 360 - 374.

[10]Corominas, J.; van Westen, C.; Frattini, P.; ... & Smith, J. Recommendations for the quantitative analysis of landslide risk. *Bulletin of engineering geology and the environment*, **2014**, *73*, 209-263.

[11]Corominas, J.; Guzzetti, F.; Lan, H.; Macciotta, R.; Marunteranu, C.; McDougall, S.; Strom, A. Revisiting landslide risk terms: IAEG commission C-37 working group on landslide risk nomenclature. *Bulletin of Engineering Geology and the Environment*, **2023**, *82*(12), 450.

[12]Ragnoli, M.; Scarsella, M.; Leoni, A.; Ferri, G.; Stornelli, V. Wireless sensor network-based rockfall and landslide monitoring systems: a review. *Sensors*, **2023**, 23(16): 7278.

[13]Tang, H. Advance and prospects of major landslides prediction and forecasting. *Bulletin of Geological Science and Technology*, **2022**, *41*(6) :1-13.

[14]Lan, Q.; Tang, J.; Mei, X.; Yang, X.; Liu, Q.; Xu, Q. Hazard Assessment of Rainfall–Induced Landslide Considering the Synergistic Effect of Natural Factors and Human Activities. *Sustainability*, **2023**, *15*(9), 7699.

[15]Murillo-García, F; Rossi, M.; Ardizzone, F.; Fiorucci, F.; Alcántara-Ayala, I. Hazard and population vulnerability analysis: a step towards landslide risk assessment. *Journal of Mountain Science*, **2017**, *14*, 1241-1261.

[16]Agboola, G.; Beni, L.; Elbayoumi, T.; Thompson, G. Optimizing landslide susceptibility mapping using machine learning and geospatial techniques. *Ecological Informatics*, **2024**, *81*, 102583.

[17]Segoni, S.; Piciullo, L.; Gariano, S. A review of the recent literature on rainfall thresholds for landslide occurrence. *Landslides*, **2018**, *15*(8), 1483-1501.

[18]Marin, R.; Garcia, E.; Aristizabal, E. Effect of basin morphometric parameters on physically-based rainfall thresholds for shallow landslides. *Engineering Geology*, **2020**, 278(1).

[19]Wang, T.; Wu, S.; Shi, J.; Xin, P. Application and validation of seismic landslide displacement analysis based on Newmark model: A case study in Wenchuan earthquake. *Acta Geologica Sinica (English Edition)*, **2013**, *87*(z1), 393-397.

[20]Liu, Q.; Zhao, Q.; Lan, Q.; Huang, C.; Yang, X.; Tang, Z.; Deng, M. Regional dynamic hazard assessment of rainfall–induced landslide guided by geographic similarity. *Bulletin of Engineering Geology and the Environment*, **2024**, 83(12), 1-22.

[21]Wu, Y.; Chen, L.; Cheng, C.; Yin, K.; Török, Á. GIS–based landslide hazard predicting system and its real–time test during a typhoon, Zhejiang Province, Southeast China. *Eng. Geol*. **2014**, *175*, 9–21.

[22]Huang, F.; Chen, J.; Fan, X.; Huang, J.; Zhou, C. Logistic regression fitting of rainfall–induced landslide occurrence probability and continuous

landslide hazard prediction modelling. *Earth Sci*. **2022**, *47*, 4609–4628.

[23] Fang, R.; Liu, Y.; Huang, Z. A review of regional landslide hazard evaluation methods based on machine learning. *Chinese Journal of Geological Hazards and Prevention*, **2021**, *32* (04): 1-8.

[24]Zhang, D; Wei, K; Yao, Y; Yang, J.; Zheng, G.; Li, Q. Capture and prediction of rainfall-induced landslide warning signals using an attention-based temporal convolutional neural network and entropy weight methods. *Sensors*, **2022**, 22(16): 6240.

[25]Xing, X.; Wu, C.; Li, J. Susceptibility Assessment for Rainfall-Induced Landslides Using a Revised Logistic Regression Method. *Natural Harzards*, **2021**, *106*, 97-117.

[26]Zeng, T.; Guo, Z.; Wang, L.; Jin, B.; Wu, F.; Guo, R. Tempo-spatial landslide susceptibility assessment from the perspective of human engineering activity. *Remote Sensing*, **2023**, *15*(16), 4111.

[27]Li, Y.; Wang, X.; Mao, H. Influence of human activity on landslide susceptibility development in the Three Gorges area. *Natural Hazards*, **2020**, *104*, 2115-2151.

[28]Ren, C.; Han, L.; Xia, T.; Xu, Q.; Zhang, D.; Sun, G.; Feng, Z. Quantitative Analysis of Human Activities and Climatic Change in Grassland Ecosystems in the Qinghai–Tibet Plateau. *Remote Sensing*, **2024**, 16(21): 4054.

[29]Zou, F.; Zhan, Q.; Zhang, W. Quantifying the impact of human activities on geological hazards in mountainous areas: evidence from Shennongjia, China. *Natural hazards*, **2018**, *90*, 137-155.

[30]Zhang, H.; Wang, Z. Human activities and natural geographical environment and their interactive effects on sudden geologic hazard: A perspective of macro-scale and spatial statistical analysis. *Applied geography*, **2022**, *143*, 102711.

[31]Liu, S.; Liu, L.; Wu, X.; Hou, X.; Zhao, S.; Liu, G. Quantitative evaluation of human activity intensity on the regional ecological impact studies. *Acta Ecologica Sinica*, **2018**, *38*(19): 6797-6809.

[32]Wen, Y. A preliminary discussion on the quantitative evaluation method of human activity intensity. *Science and Society*, **1998**, *(4)*: 56-61.

[33]de la Torre, S.; Snowdon, C.; Bejarano, M. Effects of human activities on wild pygmy marmosets in Ecuadorian Amazonia. *Biological conservation*, **2000**, *94*(2), 153-163.

[34]Brown, A. G.; Hatton, J.; O'Brien, C.; Selby, K.; Langdon, P.; Stuijts, I.; Caseldine, C. Vegetation, landscape and human activity in Midland Ireland: mire and lake records from the Lough Kinale-Derragh Lough area, Central Ireland. *Vegetation History and Archaeobotany*, **2005**, *14*, 81-98.

[35]Zhao, X. Impacts of human activity on environment in the high-cold pasturing area: A case of Gannan pasturing area. *Acta Ecologica Sinica*, **2010**, *30*(3), 141-149.

[36]Xu, Y.; Xu, X.; Tang, Q. Human activity intensity of land surface: Concept, methods and application in China. *Journal of Geographical Sciences*, **2016**, 26: 1349-1361.

[37]Singh P, Sarkar Chaudhuri A, Verma P, et al. Earth observation data sets in monitoring of urbanization and urban heat island of Delhi, India.

Geomatics, Natural Hazards and Risk, **2022**, 13(1): 1762-1779.

[38]Xu Z, Zhuang D, Yang L. Construction and application of regional quantitative model of human activity intensity. *J. Geo-Inf. Sci*, **2009**, 11: 452-460.

[39]Mao C, Ren Q, He C, et al. Assessing direct and indirect impacts of human activities on natural habitats in the Qinghai-Tibet Plateau from 2000 to 2020. *Ecological Indicators*, **2023**, 157: 111217.

[40]Quntao D, Lihui L. Summary and prospect of spatialization method of human activity intensity: taking the Qinghai-Tibet Plateau as an example. *Journal of Glaciology and Geocryology*, **2021**, 43(5): 1582-1593.

[41]Yanyan J I A, Xiaolan T. Distribution of nature protected areas and its relationship with human activity intensity in the middle and lower reaches of the Yangtze River Basin. *World Regional Studies*, **2020**, 29(4): 845.

[42]Zhang Y, Lu X, Liu B, et al. Spatial relationships between ecosystem services and socioecological drivers across a large-scale region: A case study in the Yellow River Basin. *Science of the Total Environment*, **2021**, 766: 142480.

[43]Yang H, Xu Y, Wang L, et al. Spatio-temporal variation of human activity intensity and its driving factors on the Qinghai-Tibet Plateau. *Acta Ecol. Sin*, **2023**, 43(10): 3995-4009.

[44]Liu, Y. Report on the Results of Detailed Investigation of Geological Hazards in Zhenyuan Yi Hani Lahu Autonomous County, Yunnan Province. Southwest Non-ferrous Metals Kunming Survey and Design (Institute) Co, **2015**.

[45]Diakoulaki, D.; Mavrotas, G.; Papayannakis, L. Determining objective weights in multiple criteria problems: The critic method. *Computers & Operations Research*, **1995**, *22*(7), 763-770.

[46]Miao, C.; Teng, J.; Wang, J.; Zhou, P. Population vulnerability assessment of geological disasters in China using CRITIC–GRA methods. *Arabian Journal of Geosciences*, **2018**, 11, 1-12.

[47]Wang, J.; Ma, C.; Wang, S.; Lu, X.; Li, D. Risk Assessment Model and Sensitivity Analysis of Ordinary Arterial Highways Based on RSR–CRITIC–LVSSM–EFAST. *Sustainability*, **2022**, 14(23), 16096.

[48]Shannon, C. A mathematical theory of communication. *The Bell system technical journal*, **1948**, *27*(3), 379-423.

[49]Zhang, D.; Wei, K.; Yao, Y.; Yang, J.; Zheng, G.; Li, Q. Capture and prediction of rainfall-induced landslide warning signals using an attention-based temporal convolutional neural network and entropy weight methods. *Sensors*, **2022**, 22(16), 6240.

[50]Zhu, Y.; Tian, D.; Yan, F. Effectiveness of entropy weight method in decision‐making. *Mathematical Problems in Engineering*, **2020**, (1), 3564835.

[51]Malekinezhad, H.; Sepehri, M.; Pham, Q.; Hosseini, S.; Meshram, S.; Vojtek, M.; Vojteková, J. Application of entropy weighting method for urban flood hazard mapping. *Acta Geophysica*, **2021**, 69(3), 841-854.

[52]Breiman, L. Random forests. *Machine learning*, **2001**, *45*, 5-32.

[53]Wang, Z.; Lai, C.; Chen, X.; Yang, B.; Zhao, S.; Bai, X. Flood hazard risk assessment model based on random forest. *Journal of Hydrology*, **2015**, 527, 1130-1141.

[54]Shu, B.; Liu, Y.; Wang, C.; Zhang, H.; Amani-Beni, M.; Zhang, R. Geological hazard risk assessment and rural settlement site selection using GIS and random forest algorithm. *Ecological Indicators*, **2024**, 166, 112554.

[55]Liu, Q.; Liu, H.; Lan, Q.; Li, K.; Huang, C.; Yang, X. Domain knowledge-guided intelligent recognition of multi-type potential landslides. *Knowledge-Based Systems*, **2025**, 310: 112979.

[56]Yu, B.; Xing, H.; Yan, J. Susceptibility assessment of multi-hazards using random forest—back propagation neural network coupling model: a Hangzhou city case study. *Scientific Reports*, **2024**, 14(1), 21783.

[57]Qin, Y.; Zhang, D.; Zheng, W.; Liu, B.; Gong, Z. Spatial distribution of near-fault landslides along Litang fault zones, eastern Tibetan Plateau. *Geomorphology*, **2024**, 455: 109189.

[58]Vaswani, A., Shazeer, N., Parmar, N., Uszkoreit, J., Jones, L., Gomez, A. N., ... & Polosukhin, I. Attention is all you need. *Advances in Neural Information Processing Systems*, **2017**, 30.

[59]Yuan R, Chen J. A novel method based on deep learning model for national-scale landslide hazard assessment[J]. *Landslides*, **2023**, 20(11): 2379-2403.

[60]Ni, J.; Wu, T.; Zhu, X.; ... Du, Y. Quantifying the Relationship Between Human Activities Intensity and Thawing Hazards of the Frozen Ground on the Qinghai–Tibet Plateau. *Frontiers in Earth Science*, **2022**, *10*, 845873.

[61]Xu, Y.; Xu, X.; Tang, Q. Human activity intensity of land surface: Concept, methods and application in China. *Journal of Geographical Sciences*, **2016**, *26*: 1349-1361.

[62]Huang, F.; Hu, S.; Yan, X.; … Fan, W. Landslide susceptibility prediction and identification of its main environmental factors based on machine learning models. *Bulletin of Geological Science and Technology*, **2022**, *41*(2): 79-90.

[63]Yang, Y.; Yan, X.; Wang, X. The characteristics and formation of geological hazards in Yunnan Province. *J. Catastrophol*, **2021**, *36*: 131-139.

[64]Ministry of Natural Resources of the People 's Republic of China. Specification for Geological Hazard Risk Assessment:GB/T 40112-2021. Beijing: China Standard Press, **2021**.

[65]Tan, D.; Xu, X.; Wang, L.; Xu, J.; Shi, Q. Deformation evolution and failure mechanism of rainfall-induced granite residual soil landsliding event in Northern Guangdong, China. *Landslides*, **2025**, 22(3): 925-941.

Supplementary Files

This is a list of supplementary files associated with this preprint. Click to download.

- Highlights.docx